

Complex orbital state in manganites

Ryo Maezono and Naoto Nagaosa

Department of Applied Physics, University of Tokyo, Bunkyo-ku, Tokyo 113-8656, Japan

(February 6, 2008)

Abstract

The e_g -orbital states with complex coefficients of the linear combination of $x^2 - y^2$ and $3z^2 - r^2$ are studied for the ferromagnetic state in doped manganites. Especially the focus is put on the competition among uniform complex, staggered complex, and real orbital states. As the hole-doping x increases, the real, the canted complex, and the staggered complex orbital states appears successively. Uniform complex state analogous to Nagaoka ferromagnet does not appear. These complex states can be expressed as a resonating state among the planer orbitals as the orbital liquid, accompanied by no Jahn-Teller distortion.

71.27.+a, 75.30.-m, 75.30.Et

I. INTRODUCTION

The role of the orbital degrees of freedom has recently attracted considerable interests as one of the key to understand the colossal magneto-resistance (CMR) observed in doped manganites.^{1–13} The orbital state of the conduction electrons is described as a linear combination of two wavefunctions, $|x^2 - y^2\rangle$ and $|3z^2 - r^2\rangle$, of the degenerate e_g orbitals.¹⁴ In previous studies,^{1,14} the linear combination with only real coefficients (real orbital state) has been considered. This is because theories of the orbital ordering have been developed mainly to describe the parent compounds of CMR materials,^{14–17} in which the static Jahn-Teller deformation is observed.¹⁸ Such a deformation stabilizes the real orbital state and it was reasonable to exclude the linear combination with complex coefficients (complex orbital state). Recently the orbital state in *doped* compounds is studied concerning the properties of CMR materials.^{1–13} Because the static Jahn-Teller distortion disappears in doped compounds,^{19,20} there is no reason to exclude the complex orbital state. Actually such a complex orbital state has been recently studied.^{21,22} Khomskii²¹ pointed out that the complex orbital state, $(|x^2 - y^2\rangle \pm i|3z^2 - r^2\rangle)/\sqrt{2}$, provides locally isotropic hopping intensities with the same bandwidth as the real orbital state, and might explain the isotropic properties observed in CMR compounds. Such a local isotropy cannot be realized with the uniform real orbital state.¹ A staggered ordering is therefore needed to explain the observed isotropic properties within the extent of the real orbital ordering¹ (Another proposal is the orbital liquid state, where the local isotropy is recovered by a quantum resonance between anisotropic orbital configurations, $|x^2 - y^2\rangle$, $|y^2 - z^2\rangle$, and $|z^2 - x^2\rangle$ ⁴). Based on the analogy to the Nagaoka ferromagnetism (F), Khomskii proposed that the uniform ordering (orbital F) of the complex orbital state is more stable than the staggered one (orbital AF) with real orbitals.²¹ Takahashi *et al.* investigated the possible complex orbital ordering, motivated by the analogy to the octapole ordering in heavy fermion systems with odd time reversal symmetry.²³ They found that the *staggered* ordering of the complex orbital is stable, being contrary to Khomskii's uniform one.²²

In this paper, we study the competitions among the uniform complex, staggered complex, and real orbital states by using a model of CMR compounds taking the strong on-site repulsion and the orbital degeneracy into account.¹ The complex orbital state is taken as, $\cos(\theta/2) \cdot |x^2 - y^2\rangle + i \sin(\theta/2) \cdot |3z^2 - r^2\rangle$, and the whole possibility with the continuous parameter θ is examined. With realistic parameters, the complex orbital state is more stable than the real one in the moderately doped region ($0.25 < x < 0.45$). The complex ordering changes from the canted one ($0.25 < x < 0.35$) into the staggered ($0.35 < x < 0.45$) one due to the competition between the orbital superexchange AF and the orbital Nagaoka F . The local isotropy is also realized in this complex staggered phase, where the band gap due to the doubled period brings about the energy gain exceeding the energy loss due to the narrower bandwidth than that of the uniform ordering with isotropic hopping. With increasing U/t toward the strong correlation limit, the former gain decreases whereas the latter loss increases. The staggered ordering becomes unstable in this limit, where the uniform orbital ordering wins. In this case, however, the obtained uniform ordering is not the complex one²¹ but the real one with $|x^2 - y^2\rangle$. Though the uniform complex ordering becomes more stable than the staggered complex one, it has higher energy than that of the real one. In the weak correlation limit, on the other hand, Takahashi *et al.* found that the normal metallic state becomes unstable toward the the staggered complex ordering near the quarter filling,²² with increasing U . When the Jahn-Teller coupling is further taken into account, however, it is likely that the real orbital state is stabilized, because the energy scale of the Jahn-Teller coupling becomes dominating compared with the weak U , preferring the real state.

The Jahn-Teller deformation which couples with the orbital degrees of freedom decreases in the complex canted phase and vanishes in the complex staggered phase, being consistent with the observed disappearance of the deformation.^{19,20} This complex state can be expressed as a resonating state among planer orbitals, as in the orbital liquid picture.⁴ When the resonance occurs with coherent correlations in time and space, the complex orbital ordering is obtained, meanwhile that with incoherent one corresponds to the orbital liquid state.⁴

These can be distinguished by experiments detecting the spatial correlation of the orbital symmetry, such as the anomalous X-ray scattering experiments.^{24,25} Possibilities of the phase separation and broken time-reversal symmetry are also discussed.

II. RESULTS AND DISCUSSIONS

We employ the same model as that in the previous report¹,

$$\begin{aligned}
H = & \sum_{\sigma\gamma\gamma'\langle ij\rangle} t_{ij}^{\gamma\gamma'} d_{i\sigma\gamma}^\dagger d_{j\sigma\gamma'} \\
& - J_H \sum_i \vec{S}_{t_{2g}i} \cdot \vec{S}_{e_g i} \\
& + J_S \sum_{\langle ij\rangle} \vec{S}_{t_{2g}i} \cdot \vec{S}_{t_{2g}j} + H_{\text{on site}},
\end{aligned} \tag{1}$$

where $\gamma [= a(d_{x^2-y^2}), b(d_{3z^2-r^2})]$ specifies the orbital and the other notations are standard.¹ The transfer integral $t_{ij}^{\gamma\gamma'}$ depends on the pair of orbitals (γ, γ') and the direction of the bond (i, j) .¹ The spin operator for the e_g electron is defined as $\vec{S}_{e_g i} = \frac{1}{2} \sum_{\gamma\alpha\beta} d_{i\gamma\alpha}^\dagger \vec{\sigma}_{\alpha\beta} d_{i\gamma\beta}$ with the Pauli matrices $\vec{\sigma}$, while the orbital isospin operator is defined as $\vec{T}_i = \frac{1}{2} \sum_{\gamma\gamma'\sigma} d_{i\gamma\sigma}^\dagger \vec{\sigma}_{\gamma\gamma'} d_{i\gamma'\sigma}$.¹ J_H is the Hund's coupling between e_g and t_{2g} spins, and J_S is the AF coupling between nearest neighboring t_{2g} spins. $H_{\text{on site}}$ represents the on-site Coulomb interactions between e_g electrons. Coulomb interactions induce both the spin and orbital isospin moments, and actually $H_{\text{on site}}$ can be written as

$$H_{\text{on site}} = - \sum_i \left(\tilde{\beta} \vec{T}_i^2 + \tilde{\alpha} \vec{S}_{e_g i}^2 \right). \tag{2}$$

A parameter set with $t_0 = t_{i,i+\hat{z}}^{bb} = 0.72$ eV, $\tilde{\alpha} = 8.1t_0$, and $\tilde{\beta} = 6.7t_0$ corresponds to the realistic one being relevant to the actual manganese oxides.¹ In the path-integral quantization, we introduce the Stratonovich-Hubbard fields $\vec{\varphi}_S$ and $\vec{\varphi}_T$, representing the spin and orbital fluctuations, respectively. With the large values of the electron-electron interactions above, both $\vec{\varphi}_S$ and $\vec{\varphi}_T$ are almost fully polarized.¹ The meanfield theory corresponds to the saddle point configuration of $\vec{\varphi}_S$ and $\vec{\varphi}_T$. We only consider the possibility of the complex orbital state within a F -type spin alignment in the cubic cell.

We assume the two sublattices, I and II , with F -, A -, C - and G -type alignment.¹ On each site, the orbital is specified as a linear combination of the two degenerate orbital bases, $|x^2 - y^2\rangle$ and $|3z^2 - r^2\rangle$, as

$$|\theta, \varphi\rangle = \cos \frac{\theta}{2} |x^2 - y^2\rangle + e^{-i\varphi} \sin \frac{\theta}{2} |3z^2 - r^2\rangle . \quad (3)$$

(θ, φ) is the polar angle of the corresponding isospin \vec{T} . In the limit of the infinite orbital polarization, $\tilde{\beta} \rightarrow \infty$, the uniform orbital ordering with any $|\theta, \varphi\rangle$ takes the same bandwidth, $-(3/2)t_0$. The polar angle (θ, φ) therefore controls only the dimensionality of the band structure to optimize the kinetic energy gain, leaving the bandwidth unchanged.

Previous studies^{21,22} have focused on the states with \vec{T}/\hat{e}_y as the complex orbital states. In this paper, we extend the possibility to \vec{T} lying within yz plane ($|\theta, \varphi = \pi/2\rangle$, real and pure imaginary coefficients) for the complex orbital state, whereas \vec{T} within zx plane ($|\theta, \varphi = 0\rangle$) corresponds to the real orbital state. This choice includes $|x^2 - y^2\rangle$ and $|3z^2 - r^2\rangle$ as the both ends. With finite $\tilde{\beta}$, the generalized orbital canted structure on two sublattices is examined.

Fig. 1 shows the energy values in spin F phase, optimized within the real and the complex orbital states, plotted as a function of the hole concentration x (with $J_S = 0$).

FIGURES

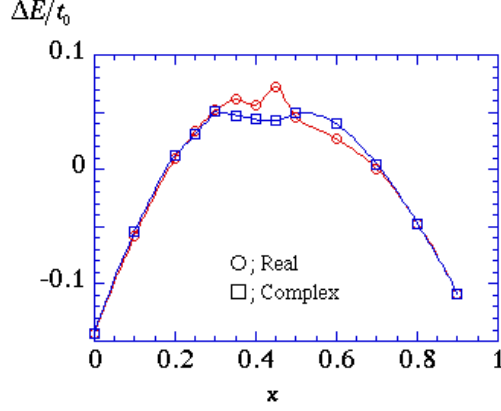


FIG. 1. Energies of the spin F phase with real and complex orbital states as a function of the hole concentration x (with $J_S = 0$).

The orbital shape specified by θ is optimized at each x . The complex orbital state is realized in the moderately doped region ($0.25 < x < 0.45$). The phase diagram as a function of x and J_S (AF interaction between t_{2g} spins) is shown in Fig. 2.

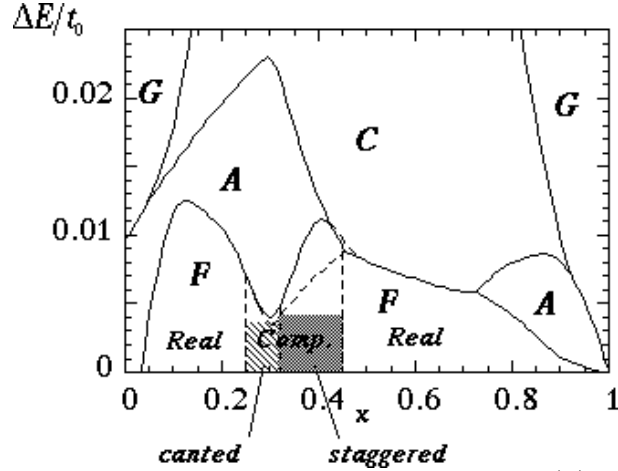


FIG. 2. Phase diagram as a function of the hole concentration (x) and the antiferromagnetic interaction between t_{2g} spins (J_S). A , C , F , and G specify the spin configuration.

In the shaded and hatched regions of the spin F phase is realized the complex orbital state. The phase boundary depicted with a broken line is that for the real orbital state, reported previously.¹

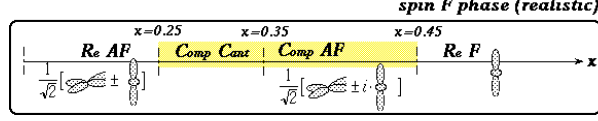


FIG. 3. The phase diagram assuming the spin F phase with realistic parameters.

Figure 3 shows the orbital phase diagram assuming the spin F phase as a function of x . The orbital ordering changes from the real staggered, the complex canted, the complex staggered, and to the real uniform one. Figure 4 shows the x -dependence of the orbital canting angle, $|\theta_{II} - \theta_I|$, for the real and the complex orbital states.

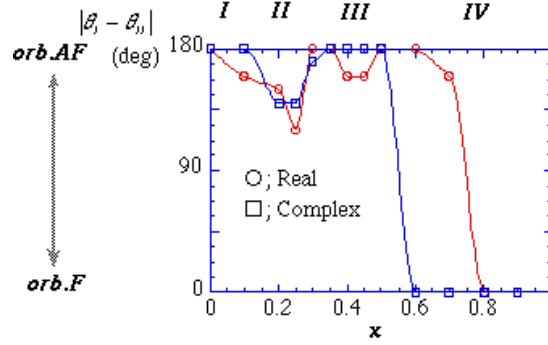


FIG. 4. x -dependence of the orbital canting angle for the real and the complex orbital states (with realistic parameters).

With increasing x , the canting angle once tends to take the orbital F ($I \rightarrow II$), but get back to AF again ($II \rightarrow III$). The canted complex state with orbital C is stable at $x = 0.25$ and 0.35 . With increasing x , the canted state changes into the staggered one for $0.35 < x < 0.45$ with $\theta_I = -\theta_{II} = \pi/2$ (orbital G) as found in ref. 22. We note that this *staggered* state also gives the locally isotropic hopping integrals, $t^x = \frac{1}{2}e^{-i\frac{2\pi}{3}}$, $t^y = \frac{1}{2}e^{i\frac{2\pi}{3}}$, and $t^z = -\frac{1}{2}$. The uniform complex state²¹ with $\theta_I = \theta_{II} = \pi/2$ and $t^{x,y,z} = -1/2$ has higher energy. With further doping (IV with $x > 0.5$), the orbital F becomes stable again, but with real coefficients.

These results can be understood as follows. The orbital superexchange AF interaction J_{AF} is represented by the shift in the center of mass of the occupied density of states (DOS), as represented by the Hamiltonian,

$$\begin{pmatrix} \varepsilon_k & \beta_{\text{eff}} \\ \beta_{\text{eff}} & \varepsilon_{k+Q} \end{pmatrix}, \quad (4)$$

with $Q = (\pi, \pi, \pi)$ being the staggered orbital momentum. Therefore J_{AF} is estimated as

$$J_{\text{AF}} \cong \frac{t^2}{\beta_{\text{eff}}} \cong \frac{t^2}{\tilde{\beta}(1-x)}, \quad (5)$$

which increases as x increases because β_{eff} is the constant $\tilde{\beta}$ times the number of electrons $(1-x)$. The ferromagnetic double exchange interaction J_{F} for the orbital moments is represented by the energy of the doped holes at the top of the occupied band, which depends on the bandwidth. The bandwidth is t for the uniform ordering whereas t^2/β_{eff} for the staggered one for $t \ll \beta_{\text{eff}}$ and small x . J_{F} is therefore given as,

$$J_{\text{F}} \sim \left(t - \frac{t^2}{\beta_{\text{eff}}} \right) \cdot x, \quad (6)$$

which represents the relative kinetic energy gain of the orbital F state measuring from that of the staggered state. It should be noted here that the notation J_{F} is rather symbolic, and the Hamiltonian is not written as $-J_{\text{F}} \sum_{ij} \vec{T}_i \cdot \vec{T}_j$. Based on these considerations, the results in Fig. 2 and 3 are interpreted as follows. Here we assume the ferromagnetic spin alignment. At $x = 0$, J_{F} vanishes meanwhile J_{AF} is finite, leading to the orbital AF . With small doping, J_{F} becomes finite, leading to the tendency toward the orbital F seen in the region II in Fig. 4. (This corresponds to the crossover from the orbital superexchange AF to the orbital double exchange (Nagaoka) F with the doping.) To understand the reentrant of the orbital AF in the region III , we note that $t^2/\beta_{\text{eff}} = t^2/\tilde{\beta}(1-x)$ increases as x , which enhances $J_{\text{AF}}(x)$ and suppresses J_{F} . Actually, the difference in the bandwidth of DOS between the uniform (orb. F) and the staggered (orb. AF) structures is hardly seen at $x = 0.3$ in Fig. 5, corresponding to $J_{\text{F}} \sim 0$.

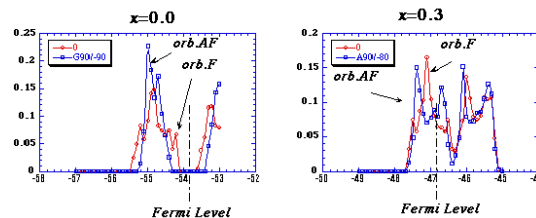


FIG. 5. Typical density of states (DOS) calculated with the orbital F and AF ordering at $x = 0$ and 0.3 .

The staggered ordering is therefore stabilized with increasing $J_{AF}(x)$ in the moderately doped region. In the heavily doped region (IV), the expression of $J_{F,AF}$ does not hold any more because $t \approx \beta_{\text{eff}}$. There the staggered ordering is unstable due to the lower bandwidth than that of the uniform one, leading to the orbital F ordering.

The competition between the real and the complex orbital states is understood as follows. The complex state is stabilized only in the moderately doped region with the advantage of the isotropic band structure. In the other region, some other mechanism is rather important than the isotropy: In the small doping region, the real state realized in Fig. 1 and 3 ($x < 0.25$) is found to be stabilized mainly due to the hybridization between the occupied and the unoccupied bands via the off-diagonal hopping integrals. In the heavily doped region, on the other hand, the low dimensional band structure, $\theta_I = \theta_{II} = 0$ (two dimensional) or π (quasi-one dimensional), is preferred where the isospin moment is along the z axis (real orbital state). This is due to the relative location between the van Hove singularity of DOS and the fermi level.¹ The fermi level with small electron concentration ($x \sim 1$, heavily doped region) is located near the band edge. The low dimensional band structure with singularities at the top and the bottom of the band can therefore lower the kinetic energy effectively with large accomodation at the singularity near the fermi level.

With increasing $\tilde{\beta}/t$, the staggered state becomes unstable because J_{AF} goes to zero whereas J_F remains to be finite. This corresponds to the recovery of the orbital Nagaoka F . One can therefore expect the uniform complex state in the small doped region with the strong correlation limit. The obtained ordering is however the *real* uniform one with $|x^2 - y^2\rangle$, not the *complex* one. The schematic phase diagram in this limit is given in Fig. 6.

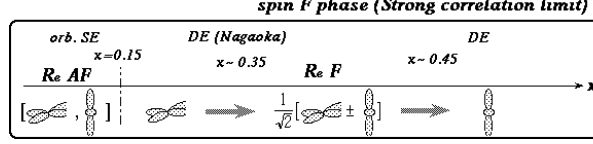


FIG. 6. Schematic phase diagram in the strong correlation limit.

This can be understood as follows. In this limit, only the DOS near the band edge matters because the bandwidth of the uniform state does not depend on the orbital shape. The DOS arises at the edge most sharply with $|x^2 - y^2\rangle$,¹ giving the largest kinetic energy gain. Orbital Nagaoka F is therefore realized with $|x^2 - y^2\rangle$ in the strong correlation limit. (It should not be confused with the real state in the small doping region with realistic parameters (Fig. 3), where the ordering is orbital AF stabilized due to the inter-band hybridization.)

Curves obtained in Fig. 1 are non-monotonic with a common tangential line contacting at two different x , where the curve is convex upwards. This means that the phase coexistence with two different concentrations has higher energy than the single phase. Therefore a spontaneous phase separation⁹ does not occur in our results.

The e_g state specified with the isospin orientation \vec{T} stabilizes the Jahn-Teller (JT) deformation expressed as $[\langle \vec{T} \rangle_z \cdot Q_u + \langle \vec{T} \rangle_x \cdot Q_v]$, where Q_u and Q_v denote the normal coordinates of the displacement of the oxygen ions Δ_α ($\alpha = x, y, z$):^{1,26}

$$Q_u = \frac{2\Delta_z - \Delta_x - \Delta_y}{\sqrt{6}}, \quad Q_v = \frac{\Delta_x - \Delta_y}{\sqrt{2}}. \quad (7)$$

The complex state realized with $0.35 < x < 0.45$ corresponds to $\vec{T} // \hat{e}_y$. With this ordering, therefore, the JT distortion does not occur. The observed disappearance of the JT distortion in the spin F metallic region^{19,20} might be explained by this type of the orbital ordering. Another theoretical proposal is the orbital liquid state where the planer orbitals, $|x^2 - y^2\rangle$, $|y^2 - z^2\rangle$, and $|z^2 - x^2\rangle$ are resonating to form a quantum liquid state.⁴ With this resonance, the local isotropy is recovered, and the JT distortion disappears on average. The complex state can actually be expressed in the form of such a resonance as,

$$\frac{1}{\sqrt{2}}|x^2 - y^2\rangle \pm i\frac{1}{\sqrt{2}}|3z^2 - r^2\rangle = \frac{\sqrt{2}}{3} \left[|x^2 - y^2\rangle + e^{\pm i2\pi/3}|z^2 - x^2\rangle + e^{\mp i2\pi/3}|y^2 - z^2\rangle \right]. \quad (8)$$

This can be regarded as a formation of the T_y -component by the resonance via the transverse components $T^\pm = T_x + iT_y$. From Eq. (8), the complex orbital ordering corresponds to the coherent (in time and space) resonance among the planer orbitals, with the relative phases $e^{\pm 2\pi/3}$ being fixed. The orbital liquid state, on the other hand, corresponds to the resonance without phase coherence. In this sense, the complex orbital state obtained here is the meanfield state akin to the orbital liquid state, and may provide a rough estimation of the energy of the latter state.⁴ Because both states give no JT distortion on average, *direct* observations of the orbital state is needed to distinguish them, not via the lattice deformation, but via the difference of the spatial orbital correlations. Several probes are available, such as the anomalous X-ray scattering,^{24,25} the X-ray charge density study by using of the maximum entropy method (MEM),²⁷ the magnetic Compton scattering,²⁸ and the polarized neutron scattering²⁹.

In summary, we studied the competitions among the uniform complex, staggered complex, and real orbital states in CMR compounds. In the moderately doped region, the complex orbital state is stabilized, where the ordering changes from the canted one ($x = 0.25, 0.3$) to the staggered one ($0.35 < x < 0.45$). This can be understood in terms of the competition among the band narrowing and the gap associating with the staggered structure, and the hybridization with the unoccupied band. The staggered complex ordering is not accompanied with the Jahn-Teller deformation. The obtained complex orbital is a coherent resonance among the planer orbitals with constant phase angles. If the coherency is lost, the state reduces to the orbital liquid state which can be distinguished by the observation of the spatial orbital correlations. The phase separation does not occur with the complex orbital state obtained here.

The authors would like to thank D. Khomskii, Y. Tokura for their valuable discussions. This work was supported by Priority Areas Grants from the Ministry of Education, Science

and Culture of Japan. R.M. is supported by Research Fellowship of the Japan Society for the Promotion of Science (JSPS) for Young Scientists.

REFERENCES

- ¹ R. Maezono, S. Ishihara and N. Nagaosa, Phys. Rev. B **57**, R13 993 (1998), *ibid.* **58**, 11 583 (1998).
- ² J. van den Brink and D. Khomskii, Phys. Rev. Lett. **82**, 1016 (1999).
- ³ Y. Endoh, K. Hirota, S. Ishihara, S. Okamoto, Y. Murakami, A. Nishizawa, T. Fukuda, H. Kimura, H. Nojiri, K. Kaneko, and S. Maekawa, Phys. Rev. Lett. **82**, 4328 (1999).
- ⁴ S. Ishihara, M. Yamanaka, and N. Nagaosa, Phys. Rev. B **56**, 686 (1997).
- ⁵ S. Okamoto, S. Ishihara, and S. Maekawa, Phys. Rev. B **61**, 451 (2000).
- ⁶ R. Kilian and G. Khaliullin, Phys. Rev. B **60**, 13 458 (1999).
- ⁷ G. Khaliullin and R. Kilian, Phys. Rev. B **61**, 3494 (2000).
- ⁸ P. Horsch, J. Jaklic and F. Mack, Phys. Rev. B **59**, 6217 (1999).
- ⁹ A. Moreo, S. Yunoki and E. Dagotto, Science **283**, 2034 (1994).
- ¹⁰ S. Yunoki, A. Moreo, and E. Dagotto, Phys. Rev. Lett. **81**, 5612 (1998).
- ¹¹ H. Shiba, R. Shiina, and A. Takahashi, J. Phys. Soc. Jpn. **66**, 941 (1997).
- ¹² A. Takahashi and H. Shiba, Euro. Phys. J. B **5**, 413 (1998).
- ¹³ P.E. de Brito and H. Shiba, Phys. Rev. B **57**, 1539 (1998).
- ¹⁴ K.I. Kugel, and D.I. Khomskii, ZhETF Pis. Red. **15**, 629 (1972). [JETP Lett. **15**, 446 (1972)]; D.I. Khomskii, and K.I. Kugel, Sol. Stat. Comm. **13**, 763 (1973).; K. I. Kugel and D. I. Khomskii, Zh. Éksp. Thor. Fiz. **79**, 987 (1980), [Sov. Phys. JETP **52**, 501 (1981)].
- ¹⁵ S. Ishihara, J. Inoue, and S. Maekawa, Physica C **263**, 130 (1996); Phys. Rev. B **55**, 8280 (1997).
- ¹⁶ R. Shiina, T. Nishitani and H. Shiba, J. Phys. Soc. Jpn. **66**, 3159 (1997).

- ¹⁷ W. Koshibae, Y. Kawamura, S. Ishihara, S. Okamoto, J. Inoue, and S. Maekawa, J. Phys. Soc. Jpn. **66**, 957 (1997).
- ¹⁸ G. Matsumoto, J. Phys. Soc. Jpn. **29**, 606 (1970).
- ¹⁹ H. Kawano, R. Kajimoto, M. Kubota, and H. Yoshizawa, Phys. Rev. B **53**, R14 709 (1996).
- ²⁰ J.F. Mitchell, D.N. Argyriou, C.D. Potter, D.G. Hinks, J.D. Jorgensen, and S.D. Bader, Phys. Rev. B **54**, 6172 (1996).
- ²¹ D. Khomskii, cond-mat/0004034 (unpublished).
- ²² A. Takahashi and H. Shiba, (unpublished).
- ²³ O. Sakai, R. Shiina, H. Shiba, and P. Thalmeier, J. Phys. Soc. Jpn. **66**, 3005 (1997), *ibid* **67**, 941 (1997).
- ²⁴ Y. Murakami, H. Kawada, M. Tanaka, T. Arima, Y. Moritomo and Y. Tokura, Phys. Rev. Lett. **80**, 1932 (1998).
- ²⁵ Y. Murakami, J. P. Hill, D. Gibbs, M. Blume, I. Koyama, M. Tanaka, H. Kawata, T. Arima, Y. Tokura, K. Hirota, and Y. Endoh, Phys. Rev. Lett. **81**, 582 (1998).
- ²⁶ J. Kanamori, J. Appl. Phys. **31**, 14S (1960).
- ²⁷ M. Takata, E. Nishibori, K. Kato, M. Sakata and Y. Moritomo, J. Phys. Soc. Jpn. **68**, 2190 (1999).
- ²⁸ A.Koizumi, N. Sakai, N. Shirai, and M. Ando, J. Phys. Soc. Jpn. **66**, 318 (1997).
- ²⁹ J.Akimitsu and Y.Ito, J. Phys. Soc. Jpn. **40**, 1621 (1976).
- ³⁰ B.S. Shastry, B.I. Shraiman, and R.R.P. Singh, Phys. Rev. Lett. **70**, 2004 (1993).